THE ASTROPHYSICAL JOURNAL, 567:L169–L172, 2002 March 10
© 2002. The American Astronomical Society. All rights reserved. Printed in U.S.A.

MEASUREMENT OF EMISSION CROSS SECTIONS FOR $n = 3 \rightarrow 2$ LINES IN Li-LIKE Fe^{23+}

H. CHEN, P. BEIERSDORFER, AND J. H. SCOFIELD
Lawrence Livermore National Laboratory, 7000 East Avenue, Livermore, CA 94550
K. C. GENDREAU, K. R. BOYCE, G. V. BROWN, R. L. KELLEY, F. S. PORTER, C. K. STAHLE, AND A. E. SZYMKOWIAK
NASA Goddard Space Flight Center, Code 680, Greenbelt, MD 20771
AND
S. M. KAHN
Columbia Astrophysics Laboratory, Columbia University, 550 West 120th Street, New York, NY 10027
Received 2001 July 5; accepted 2002 January 31; published 2002 February 21

ABSTRACT

We report measurements of emission cross sections for iron L-shell $3 \rightarrow 2$ lines in Fe^{23+} performed on the electron beam ion trap EBIT-II using a combination of a crystal spectrometer and the spare 6×6 element X-Ray Spectrometer microcalorimeter from the *Astro-E* X-ray satellite mission. Use of the microcalorimeter enables for first time the normalization of line emission cross sections, i.e., effective electron impact excitation cross sections that include radiative cascades, to the well-established cross section of radiative electron capture, thus allowing the normalization of relative line intensity measurements using crystal spectrometers.

Subject headings: atomic data — atomic processes — methods: laboratory — X-rays: general

On-line material: color figure

1. INTRODUCTION

Accurate iron L-shell atomic data are important for the interpretation of astrophysical observations (Kahn & Liedahl 1990). The need for accurate data has become crucial following the availability of high-resolution X-ray data collected by the *X-Ray Multi-Mirror Mission* (*XMM-Newton*) and the *Chandra X-Ray Observatory*. To address this need, the laboratory astrophysics program utilizing the electron beam ion trap facility EBIT-II at the Lawrence Livermore National Laboratory has produced detailed sets of Fe L-shell line positions and relative line intensities (Brown et al. 1999a). It also has measured a number of line emission cross sections (Gu et al. 1999b, 2001), where the Fe L-shell line emission measurements were normalized to theoretical calculations.

Although such a normalization can be fairly reliable, especially at high electron-ion collision energies, the accuracy of electron scattering calculations is limited to 15%–30% (e.g., Zhang & Sampson 1989)—and may be much worse, by factors of 2 or more, if the levels are affected by configuration interactions. A more reliable method is to normalize the measurements to radiative electron capture, i.e., radiative recombination (RR). This is because RR, the inverse of photon ionization, is the simplest atomic scattering process and at high energy involves only one electron and one photon. An RR X-ray is produced by capturing a free electron into a bound level. The X-ray photon has an energy equal to the sum of the free electron energy and ionization potential of the level into which the electron is captured. At high electron energies, the RR cross sections are known from both calculations and synchrotron measurements to an accuracy of 3%–5% (Saloman, Hubbell, & Scofield 1988).

Normalization to RR has been used for the measurements of effective excitation cross sections (Chantrenne et al. 1992; Wong, Beiersdorfer, & Vogel 1995) for K-shell ions, but the energy resolution ($\geq$160 eV) of the broadband X-ray detectors used in these studies was not sufficient to determine the emission cross section of L-shell ions. This situation has changed with the advent of microcalorimeter detectors that have energy resolution better than 25 eV (Le Gros et al. 1995; Kelley et al. 1999; Stahle et al. 1999).

Recently, the spare X-Ray Spectrometer (XRS) microcalorimeter detector (Kelley et al. 1999; Porter et al. 1999; Audley et al. 1999; Gendreau et al. 1999; Boyce et al. 1999) from the Astro-E mission (Ogawara et al. 1998) was installed on EBIT-II (Porter et al. 2000). The XRS has unique features that enabled the present measurements. These are a combination of high effective area (12.5 mm^2), electronic stability, and microsecond time resolution absent in other devices. This combination is needed because the RR cross sections are about 3 orders of magnitude smaller than the electron impact excitation cross sections of L-shell ions, making it necessary to observe with large-area detectors for long times without electronic gain drift. In this Letter we report our results for the three Fe XXIV $n = 3 \rightarrow 2$ lines ($3p_{3/2} \rightarrow 2s_{1/2}$, $3p_{1/2} \rightarrow 2s_{1/2}$, and $3d_{5/2} \rightarrow 2p_{3/2}$) that in previous measurements were normalized to theoretical values (Gu et al. 1999b).

2. EXPERIMENT

Our experiments were carried out on the EBIT-II device (Levine et al. 1988). In addition to the spare XRS detector, we used the flat-crystal spectrometer described by Brown, Beiersdorfer, & Widmann (1999b). The crystal spectrometer is needed to resolve individual L-shell Fe lines. It employed a $50 \times 25 \times 25$ mm^3 thallium acid phthalate crystal at a 26° Bragg angle, giving wavelength coverage from 9.5 to 12 Å (0.9–1.2 keV). It had a resolving power of 385 (FWHM of 2.6 eV at a photon energy of 1 keV). For comparison, the microcalorimeter has moderate resolution: FWHM of about 9 eV at a photon energy of 1 keV. However, its bandwidth of 0.3–10 keV allows simultaneous coverage of both Fe L-shell line emission (near 1 keV) and RR radiation (at 4–5 keV) at the electron beam energies used in our experiment. Normalizing the L-shell line emission to RR requires knowledge of the intensity response of the XRS. A detailed calibration of its response was obtained before the EBIT-II experiments (Gendreau et al. 1999; Audley et al. 1999). This includes the transmission of the five thin-foil filters (four

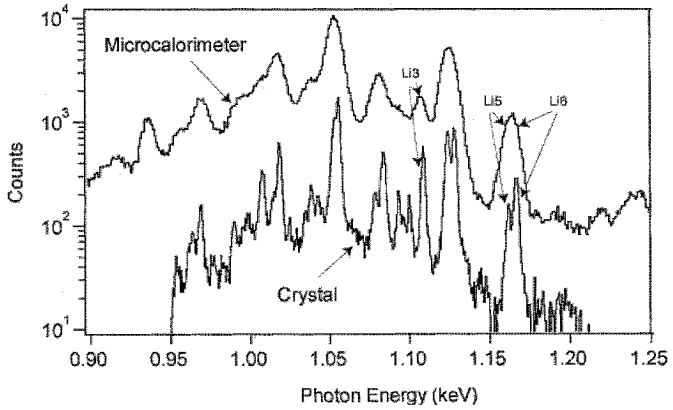

FIG. 1.—Fe spectra taken by the crystal spectrometer and the microcalorimeter at an electron beam energy of 2.1 keV. The three Fe XXIV $3 \rightarrow 2$ 1ines marked are Li3 ($3p_{3/2} \rightarrow 2s_{1/2}$), Li5 ($3p_{1/2} \rightarrow 2s_{1/2}$), and Li6 ($3d_{5/2} \rightarrow 2p_{3/2}$).

A1/polyimide filters, with thicknesses of 545 Å/795 Å, 498 Å/775 Å, 1023 Å/1085 Å, and 1023 Å/1085 Å; the fifth filter is a 1 μm thick Be foil) used to separate the XRS and EBIT-II vacua as well as to reduce thermal loading on the XRS. Also, during the experiment we checked the filter response to look for ice buildup and to account for any changes (G. V. Brown et al. 2002, in preparation).

Low-charge Fe was injected into EBIT-II using a metal vapor vacuum arc source (Brown et al. 1986). The ions were ionized by the beam and trapped for about 5 s. Then the trap was emptied and filled anew. We chose to analyze only those data acquired after ionization equilibrium was reached, i.e., data recorded at least 1 s after the injection.

Measurements were made at three electron beam energies: 2.1, 2.5, and 3.0 keV. These energies are 2–3 times higher than the threshold for direct excitation. This prevents contributions to the line emission from dielectronic recombination and resonance excitation, ensuring the line emission primarily comes from direct electron impact excitation and radiative cascades from higher lying levels. Our method determines the emission cross section of the Fe L-shell lines, i.e., the net cross section of *all* line formation processes that contribute to the line emission at given electron energy.

Typical Fe spectra from both instruments are shown in Figure 1. The wavelength scale was established using line emission previously measured on EBIT-II (Brown et al. 1999a) and the Princeton Large Torus tokamak (Wargelin et al. 1998). Most of the Fe $3 \rightarrow 2$ L-shell lines observed with the crystal spectrometer were resolved, while only a few of those observed with the microcalorimeter were resolved, illustrating the need to operate both simultaneously in the laboratory.

The RR spectra measured by the XRS microcalorimeter are shown in Figure 2 for electron beam energies of 2.1 and 3.0 keV. The RR X-rays were produced by the capture of beam electrons into the fine-structure levels of the ground states of Fe^{20+} through Fe^{23+} ions. Unlike in a Maxwellian plasma, RR X-rays excited by a nearly monoenergetic electron beam form distinct, resolved features. From the data we determine the energy spread of the electron beam to be 40 ± 2 eV for the 2.1 keV electron beam and 44 ± 3 eV for the 3.0 keV beam. This width is larger than the fine-structure separations of the individual RR lines. These separations are as little as 10 eV (see Fig. 2, *bottom panel*, where the individual RR lines are indicated by thin lines), and therefore we cannot resolve them in the XRS spectrum. However, the separations of the RR features among different charge states are typically more than twice the electron beam width and can be distinguished clearly in the XRS spectrum.

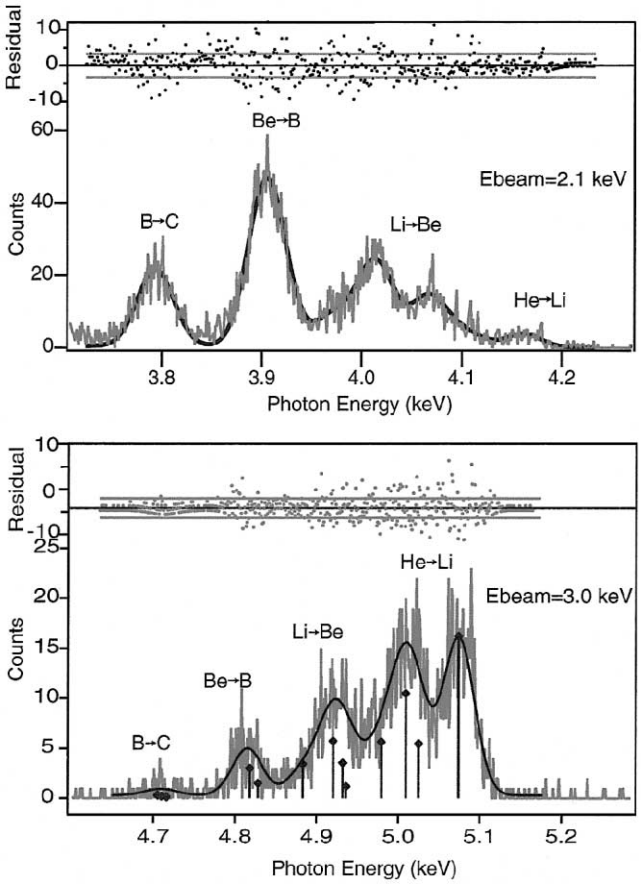

FIG. 2.—Fe RR spectrum measured with the microcalorimeter at electron beam energies of 2.1 keV (*top panel*) and 3.0 keV (*bottom panel*). Also shown are spectral fits and residuals. Position and relative intensity of individual transitions included in the fitting are indicated as thin lines and markers in the 3.0 keV spectrum. [*See the electronic edition of the Journal for a color version of this figure.*]

3. DATA ANALYSIS AND RESULTS

For charge state i, the line intensity can be described by

$$I = G(E)\eta T\sigma v_e(E) \int n_e(r) n_i(r) d^3r. \quad (1)$$

In the case of the microcalorimeter measurements, G represents the effects of the angular distribution of the polarized radiation, η is the quantum efficiency of the detector, and T is the filter transmission; σ is the emission cross section of the line, and v is the electron impact velocity. The integral of the electron density n_e and ion density n_i is over the emitting volume seen by each instrument. For the microcalorimeter, $G = 3/(3 - P)$ for electric dipole transition, where P is the degree of linear polarization (Beiersdorfer et al. 1996). We experimentally measured I, η, and T. The polarization P was calculated using the code of Zhang, Sampson, & Clark (1990). We also took into account the depolarizing effect due to the transverse beam energy of ~200 eV (Gu, Savin, & Beiersdorfer 1999a). The volume integral needs to be determined by normalizing to the RR intensity.

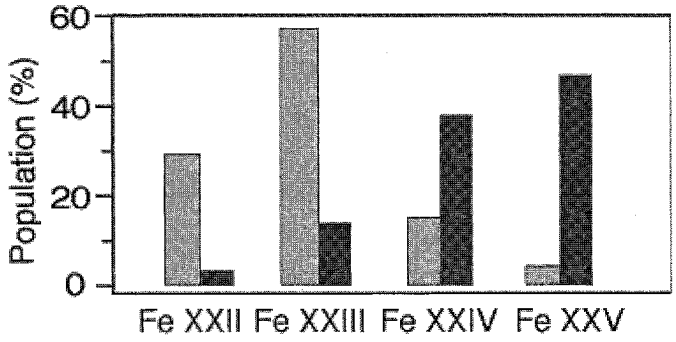

FIG. 3.—Relative Fe charge balance in EBIT-II at two electron beam energies: 2.1 keV (*gray*) and 3.0 keV (*black*).

The RR intensities for each charge state are given by

$$I^{\rm RR} = \sum_j G_j^{\rm RR}(E)\eta_j^{\rm RR}T_j^{\rm RR}\sigma_j^{\rm RR}\nu_e(E)\int n_e(r)n_i(r)d^3r. \quad (2)$$

The summation is over the fine structure of a given ion, represented by subscript j. For example, in the case of electron capture by Li-like Fe to produce Be-like Fe, the ground-state fine structure includes $2s_{1/2}^2$ ($J = 0$), $2s_{1/2}2p_{1/2}$ ($J = 0$, $J = 1$), and $2s_{1/2}2p_{3/2}$ ($J = 1$, $J = 2$). By measuring the RR and line emission intensity simultaneously with the same instrument, we can eliminate the volume integral and solve for the line emission cross section:

$$\sigma = \frac{\sum_j G_j^{\rm RR}\eta_j^{\rm RR}T_j^{\rm RR}\sigma_j^{\rm RR}}{G\eta T}\frac{I}{I^{\rm RR}}. \quad (3)$$

Because the XRS could not fully resolve the $3 \rightarrow 2$ transition lines, we had to rely on the crystal spectrometer to determine the individual line intensities. In this circumstance, the volume integral cannot be eliminated by taking the ratio of equations (1) and (2) because two separate instruments were used for the RR and line emission measurements. Instead, we first need to extract the line intensity from the crystal data and relate it to that of the microcalorimeter measurement:

$$I_{\rm X} = A\frac{G_{\rm X}T_{\rm X}\eta_{\rm X}}{G_cT_c\eta_c}I_c, \quad (4)$$

where c stands for crystal and X for XRS. For the crystal spectrometer, factor G includes not only the effect of the angular distribution of the polarized radiation but also the response of the crystal reflectivity to polarized radiation (Beiersdorfer et al. 1992, 1996; Gu et al. 1999b). For the crystal reflectivity, we used a value averaged between perfect and mosaic crystals (Henke, Gullikson, & Davis 1993). The geometry factor A represents the ratio of the plasma volume in the field of view of the crystal and the microcalorimeter. We determine this factor from the responses of the crystal spectrometer and microcalorimeter using the two Fe XXIV lines $1s^23p_{1/2} \rightarrow 1s^22s_{1/2}$ and $1s^23p_{3/2} \rightarrow 1s^22s_{1/2}$ (labeled as Li5 and Li6 in Fig. 1) as common references. These two lines are well isolated from the other lines, and their intensities can be determined accurately.

$I^{\rm RR}$ is determined by fitting the RR emission using the relative position and intensities of each RR fine-structure configuration known from theory. We achieved very reliable spectral fits for the RR spectra at all three energies.

It is interesting to note that we have different charge balances in the trap at these three electron energies, and this information can be extracted from the RR intensities. From equation (2) we can infer the ionization balance from spectral fits to the RR data:

$$n_i \propto \frac{I^{\rm RR}}{\sum_j G_j^{\rm RR}(E)\eta_j^{\rm RR}T_j^{\rm RR}\sigma_j^{\rm RR}}. \quad (5)$$

The results are shown in Figure 3 for the beam energies 2.1 and 3.0 keV. The dominant ion in the trap was Fe XXIII at an electron beam energy at 2.1 keV, while Fe XXIV and Fe XXV ions became dominant at an electron beam energy of 3.0 keV.

The results of the emission cross sections for the three Fe XXIV lines are summarized in Table 1. The cross sections from the present measurement are compared with the theoretical values of the cross sections from ***R***-matrix calculations by Berrington & Tully (1997). These cross sections have been used by Gu et al. (1999b) for normalizing their line intensity measurements. The emission cross sections from Berrington & Tully (1997) include cascade contributions from $n = 3$ and 4. In principle, cascades from all n levels can contribute to the measured emission cross section, whereby the total contribution from all cascades is estimated to be about 15% (Gu et al. 1999b). Adding cascade contributions from $n \geq 5$ to the calculated values will increase the calculated emission cross sections. Because the overall ***R***-matrix calculations are already somewhat higher than the measured data, this will only increase the difference, albeit by only a small amount.

Table 2 gives a summary of the error contributions for the three lines. The error analysis included the statistical fitting error of the line intensities, filter transmissions, and detector responses for the crystal spectrometers and the microcalorimeter. We also estimated the errors associated with accounting for the angular distributions and crystal reflectivities. An additional error comes from determining the appropriate intensity of the background level, given the high density of the unresolved weak Fe lines in the XRS spectra. In the analysis, we estimated the upper and lower limit of the background level to assess this error. The total error given is the quadrature summation of all individual errors. At 2.1 and 3.0 keV, the error is about 10%, while at 2.5 keV it is close to 20% because of lower counting statistics. The error associated with proper determina-

TABLE 1

MEASURED EMISSION CROSS SECTIONS FOR THREE Fe XXIV LINES AT THREE ELECTRON ENERGIES

	2.1 keV		2.5 keV		3.0 keV	
TRANSITIONS	Present Measurements	Theory Values	Present Measurements	Theory Values	Present Measurements	Theory Values
Li6: $3p_{3/2} \rightarrow 2s_{1/2}$	3.1 (0.4)	4.2	3.4 (0.7)	3.9	3.4 (0.3)	3.7
Li5: $3p_{1/2} \rightarrow 2s_{1/2}$	1.8 (0.2)	2.3	1.8 (0.4)	2.0	2.1 (0.2)	2.1
Li3: $3d_{5/2} \rightarrow 2p_{3/2}$	6.3 (0.6)	6.0	4.5 (0.9)	5.7	5.0 (0.5)	5.2

NOTE.—All emission cross sections are in units of 10^{-21} cm^2. Theory values are from Berrington & Tully 1997.

TABLE 2
ERROR ANALYSIS (IN PERCENT) OF THE EMISSION CROSS SECTIONS AT THREE ELECTRON ENERGIES

	2.1 keV								
TRANSITION	Statistics (Line)	Statistics (RR)	Polarization	Quantum Efficiency (Crystal)	Quantum Efficiency (XRS)	Background Level	Total	2.5 keV (Total)	3.0 keV (Total)
Li6: $3p_{3/2} \rightarrow 2s_{1/2}$	6	2.2	2	0.1	<5	6.1	10.3	17.4	8.7
Li5: $3p_{1/2} \rightarrow 2s_{1/2}$	7	2.2	0	0.1	<5	6.1	10.8	17.7	8.5
Li3: $3d_{5/2} \rightarrow 2p_{3/2}$	3	2.2	2	0.1	<5	6.1	8.9	17.2	8.7

tion of the background level was the largest contributor to the total error: it is about 8%–10% for measurements at beam energies at 2.1 and 3.0 keV and 17% for those at 2.5 keV.

4. SUMMARY

The combination of high-resolution crystal spectrometer and broadband large-area microcalorimeter measurements enables us to determine the emission cross sections of L-shell Fe lines by direct normalization to the RR cross section. We reported the results for several $3 \rightarrow 2$ transitions from Fe XXIV at three electron energies. Our results validate distorted wave and ***R***-matrix calculations used for normalization in our earlier measurements. The largest uncertainties in the measurements were caused by the difficulty of determining the background level in the XRS data because of the presence of many unresolved, weak lines. The good agreement with theory in this case is in part expected owing to the simplicity of the Fe XXIV ion: the single-valence electron greatly reduces the complexity of calculation. The measurement technique we have demonstrated will enable us to measure more complex ions, e.g., C-like Fe XXI, which has a very complex atomic structure and represents a challenge to calculation methods, but which is observed in astrophysical spectra.

This work was performed under the auspices of the US Department of Energy by the University of California Lawrence Livermore National Laboratory under contract W-7405-Eng-48 and was supported by NASA Space Astrophysics Research and Analysis grants to the Lawrence Livermore National Laboratory, the Goddard Space Flight Center, and Columbia University.

REFERENCES

Audley, M. D., et al. 1999, Proc. SPIE, 3765, 751
Beiersdorfer, P., Phillips, T. W., Wong, K. L., Marrs, R. E., & Vogel, D. A. 1992, Phys. Rev. A, 46, 3812
Beiersdorfer, P., et al. 1996, Phys. Rev. A, 53, 3974
Berrington, K. A., & Tully, J. A. 1997, A&AS, 126, 105
Boyce, K. R., et al. 1999, Proc. SPIE, 3765, 741
Brown, G. V., Beiersdorfer, P., Liedahl, D. A., Widmann, K., & Kahn, S. M. 1999a, LLNL Rep. UCRL-JC-136647
Brown, G. V., Beiersdorfer, P., & Widmann, K. 1999b, Rev. Sci. Instrum., 70, 280
Brown, I. G., Galvin, J. E., MacGill, R. A., & Wright, R. T. 1986, Appl. Phys. Lett., 49, 1019
Chantrenne, S., Beiersdorfer, P., Cauble, R., & Shneider, M. B. 1992, Phys. Rev. Lett., 69, 265
Gendreau, K. C., et al. 1999, Proc. SPIE, 3765, 137
Gu, M. F., Kahn, S. M., Savin, D. W., Bahar, E., Beiersdorfer, P., Brown, G. V., Liedahl, D. A., & Reed, K. J. 2001, ApJ, 563, 462
Gu, M. F., Savin, D. W., & Beiersdorfer, P. 1999a, J. Phys. B, 32, 5371
Gu, M. F., et al. 1999b, ApJ, 518, 1002
Henke, B. L., Gullikson, K. M., & Davis, J. C. 1993, At. Data Nucl. Data Tables, 54, 181
Kahn, S. M., & Liedahl, D. A. 1990, in Iron Line Diagnostics in X-Ray Sources, ed. A. Treves, G. C. Perola, & L. Stella (Berlin: Springer), 3
Kelley, R. L., et al. 1999, Proc. SPIE, 3765, 114
Le Gros, M., Silver, E., Beiersdorfer, P., Crespo López-Urrutia, J., & Widmann, K. 1995, EBIT Annual Rep. (LLNL Rep. UCRL-ID-124429), 22
Levine, M. A., Marrs, R E., Henderson, J. R., Knapp, D. A., & Schneider, M. B. 1988, Phys. Scr., T22, 157
Ogawara, Y. 1998, in IAU Symp. 188, The Hot Universe, ed. K. Koyama, S. Kitamoto, & M. Itoh (Dordrecht: Kluwer), 75
Porter, F. S., et al. 1999, Proc. SPIE, 3765, 729
———. 2000, Proc. SPIE, 4140, 407
Saloman, E. B., Hubbell, J. H., & Scofield, J. H. 1988, At. Data Nucl. Data Tables, 38, 1
Stahle, C. K., et al. 1999, Proc. SPIE, 3765, 82
Wargelin, B. J., Beiersdorfer, P., Liedahl, D. A., Kahn, S. M., & von Goeler, S. 1998, ApJ, 496, 1031
Wong, K. L., Beiersdorfer, P., & Vogel, D. A. 1995, Phys. Rev. A, 51, 1214
Zhang, H. L., & Sampson, D. H. 1989, At. Data Nucl. Data Tables, 43, 1
Zhang, H. L., Sampson, D. H., & Clark, R. E. H. 1990, Phys. Rev. A, 41, 198